Proceedings of 11th International Materials Symposium, April 19-21, 2006, Denizli, Türkiye

OPEN CELL Ti6Al4V FOAMS FOR BIOMEDICAL APPLICATIONS

BİYOMEDİKAL UYGULAMALAR İÇİN AÇIK GÖZENEKLİ Ti6Al4V KÖPÜKLER

A. Hizal, E. Akar & M. Güden
Izmir Institute of Technology, Izmir, TURKEY, 35430

ABSTRACT: Sintered Ti6Al4V alloy foams were prepared using atomized spherical powders in the porosity range of 52-72 % using a space holder. Powder-space holder mixture was cold compacted at 200, 300, 400, 500 and 700 MPa compaction pressures and then sintered at 1200 °C for 2 h and 1300 °C for 2, 4 and 6 h. The porosity level and mean pore sizes of the sintered foams were determined as function of the compaction pressure and sintering temperature and duration. The compression strength and deformation behavior of the foams were investigated.
Keywords: Powder metallurgy; Ti6Al4V; Porous material; Sintering

ÖZET: Sinterlenmiş Ti6Al4V toz alaşım köpükler, %52-72 gözenek aralığında, küresel tozlar ve boşluk yapıcı madde kullanılarak hazırlanmıştır. Toz-boşluk yapıcı madde karışımı 200, 300, 400, 500 ve 700 MPa basınçlarda soğuk preslenlenerek, 1200 °C de 2 saat ve 1300 °C de 2, 4 ve 6 saat süresince sinterlenmiştir. Sinterlenmiş köpüklerin gözenek miktarları ve ortalama gözenek boyutları uygulanan presleme basıncı ve sinterleme sıcaklığı ve sürelerine bağlı olarak belirlenmiştir. Hazırlanan köpüklerin mukavemetleri ve basma davranışları incelenmiştir.
Anahtar Kelimeler: Toz metalurjisi; Ti6Al4V; Gözenekli malzemeler; Sinterleme.

1 INTRODUCTION

Ti and its alloys have been known to show good corrosion resistance and fatigue behavior and excellent biocompatibility to human body. These properties made Ti and its alloys one of the most important class of materials in orthopedic and dental implant applications. Similar to the most bulk metallic implant materials currently used in orthopedic applications, Ti and its alloys suffer from the problems of interfacial stability with host tissues and biomechanical mismatch of elastic modulus. These problems stem from weak bonding of implant to the adjacent bone and high elastic modulus of bulk metallic implants. Developments in tissue engineering have demonstrated that those problems can be solved using porous implant components based on biocompatible metallic materials, simply by providing better interaction with bone. This is partly due to higher degree of bone growth into porous surfaces and higher degree of body fluid transport through three-dimensional interconnected array of pores [1], leading to improved implant fixation. Furthermore, relatively low elastic modulus of porous metals as compared with those of bulk metals is expected to reduce the extent of stress shielding, which causes the well-known *implant loosening*, and hence to prolong implant life-time [2].

Two methods of Ti-based porous implant structures and/or coatings are currently under investigation. The first process is based on the sintering of Ti and/or Ti6Al4V powder compacts preformed under pressure. Using this method, porous Ti and Ti6Al4V compacts potentially to be used in biomedical applications were previously prepared successfully with interconnected pores [3, 4, 5]. The method allows a direct near net-shape fabrication of porous implant components having elastic modulus comparable with that of natural bone and with a relatively homogeneous pore structure and low level of porosity (<40%). The pore size ranged between 50 and 200 μm, depending on the powder size and compaction pressure used [3, 4, 5]. It was further shown that the utilization of Ti6Al4V powder increased the strength of the compacts significantly as compared with pure Ti powder [5]. The optimum pore size ranges required for the attachment and proliferation of new bone tissue and the transport of body fluids are however given to be between 200 and 500 μm [6]. To reach optimum pore size range, a space holder having the particle size in the optimum pore size range for the bone tissue attachment is used in the powder compacts. It was noted that for the preparation of highly porous foam parts, the particle size of metal powder should be smaller than the average particle size of space holder [3]. A Particle size smaller than 150 μm is normally considered to be sufficient for the homogeneous coating of 200-500 μm size space holder particles with Ti powder. Furthermore, the

consolidation pressure used for the compaction of metal powder-space holder mixture must be high enough for the preparation of mechanically strong compacts that would retain their geometry throughout the foaming process. The compaction of Ti powder is usually conducted under a uniaxial pressure ranging between 100 and 200 MPa, while higher pressures, or a binder material, may be required for the compaction of the harder Ti6Al4V powder.

This experimental study was conducted to produce stronger Ti6Al4V foams that can potentially be used in biomedical applications including human cortical bone replacement and spinal cages for spine surgery. The experimental work presented focused on the determination of Ti6Al4V process parameters and the compression mechanical properties of the foams as function of porosity.

2 MATERIALS AND TESTING METHODS

The processing steps of space holder method are schematically presented in Figure 1. The process starts with mixing of metal powders with a suitable space holder material, followed by a compaction step (e.g. uniaxial and isostatic pressing) that produces metal powder-space holder mixture compact. The green compact is then heat treated at a relatively low temperature to release the space holder, resulting in an unfired open cell foam metal structure. Finally, the compact is sintered at relatively high temperatures to provide structural integrity. This method allows a direct near net-shape fabrication of foamed implant components with a relatively homogeneous pore structure and a high level of porosity (60-80%).

The cylindrical foam samples were prepared using atomized spherical Ti6Al4V alloy powder. The particle size of powder ranged between 23 and 90 μm with a mean particle size of 70.5 μm (Fig. 2). The chemical composition of Powder is complied with ASTM 1580-1 standard [7] as tabulated in Table 1. The microstructure of as-received Ti6Al4V powder is composed of martensitic α known as acicular (needle like) α (Fig. 3). The needle-like microstructure is resulted from atomization process due to quenching after heat treatment above β-transition temperature. The particle size of the space holder ranged between 315 and 500 μm (Fig. 4).

Table 1 ASTM standard for Ti6Al4V powder chemical composition.

Element	Al	V	O	Fe	C
ASTM F1580-01	5.5~6.75	3.5~4.5	0.2	0.3	0.08
Testing Results	6.13	3.89	0.17	0.11	0.02

Before compaction, Ti6Al4V powder was mixed with 52, 62 and 72 % (by volume) of ammonium bicarbonate (space holder) and PVA solution as the binding material. The mixture was then compacted at room temperature inside a steel die. The green compacts were 10 mm in length and 15 mm in diameter. It was found that without using a binder the powder could not be shaped until about the pressures of 200 MPa; therefore, PVA solution 10% by volume was used as the binding material in an amount of 10% by weight. Compaction pressures investigated were 200, 300, 400, 500 and 700 MPa. During heating the compact to the sintering temperature, the space holder was removed at 200 °C for 5 hours. The sintering of compacts was performed in a tightly enclosed horizontal tube furnace under the high purity (99.998%) Ar atmosphere at temperatures 1200 and 1300 °C for 2, 4 and 6 h. The sintering temperature and time were chosen based on the previous sintering studies of Ti foam and powder compacts [8, 9]. The compacts were inserted into the furnace at room temperature inside an enclosed Ti6Al4V box on a graphite plate which prevented the bonding between Ti6Al4V box and foams. The compacts were heated and cooled with a rate of 5 °C per min. In the heating cycle, the foams were kept at 450 °C for ½ hour in order to allow the burning of the binder.

Porosity levels of sintered foams were determined using the Archimedes' method after coating the surface of the foams with paraffin to prevent penetration of water into the pores. Quasi-static compression tests were performed on the cylindrical foam samples using a displacement controlled SHIMADZU AG-I universal tension-compression test machine. Eccentric compression test plate was used in all tests in order to prevent shear forces formed by uneven surfaces of the test specimens. Tests were performed at a cross-head speed of 2 mm min^{-1} corresponding to a strain rate of $2x10^{-3}$ s^{-1}, respectively. During compression test, the test plates and surfaces of the samples were lubricated in order to reduce the friction between sample and the test plates. At least three tests were conducted for each set of powder samples. Elastic modulus, yield stress, ultimate compressive stress and failure strain values were determined from the stress-strain curves. The measured strain values were corrected with the compliance of the compression test machine.

3 RESULTS AND DISCUSSION

The porosity levels of the foams prepared are tabulated in Table 2 together with applied compaction pressures, space holder volume % and sintering temperature and duration. Increasing compaction

pressure and sintering temperature and sintering duration increase the relative density of foams by providing higher contact areas between particles, leading to decrease in the final foam porosity values. The porosity levels of the foams vary between 49% and 73% (Table 2).

The compressive stress-strain curves of the prepared foams compacted at different compaction pressures and sintered at 1200 °C for 2 h are shown in Figure 5. The maximum compressive stress is around 40 MPa and its value decreases as the compaction pressure decreases. It is also noted that the foams show relatively low elastic moduli values, ranging between of 0.52 – 1.18 GPa, depending on the applied compaction pressure. The porosity levels of the foams range between 62 and 64% as listed in Table 2. The increase in the compressive stress of the foams with increasing compaction pressure may be attributed to increased contact area between the particles. However, the brittle failure mode of foams dictates that the bonding area between the sintered particles is not large enough or the bonding between particles is not strong enough to induce a ductile failure mode of deformation composing of the regions of elastic deformation and cell collapse in the stress-strain curve.

Table 2. Compaction pressures, space holder ratio, sintering temperature, sintering time, porosity and mean pore size of the prepared foams.

Compaction Pressure (MPa)	Space Holder Volume, %	Sintering Temp (°C)	Sintering duration (h)	Porosity (%)
200	62	1200	2	64
300	62	1200	2	63
400	62	1200	2	63
500	62	1200	2	62
300	62	1300	2	61
500	62	1300	2	60
700	62	1300	2	58
700	62	1300	4	57
500	62	1300	4	61
500	62	1300	6	58
500	72	1300	6	73
500	52	1300	6	49

The compressive stress-strain curves of foams sintered at 1300 °C for 2 h are shown sequentially in Figure 6 and 7 for 500 and 700 MPa cold compaction pressures, respectively. Increasing sintering temperature comes with several effects in the compression behavior of the foam. First at low compaction pressures, 300 and 500 MPa although foam still shows relatively brittle behavior the compressive stresses increases greatly as compared with that of the samples sintered at 1200 °C. The compressive stress ranges between 50 and 80 MPa for the compaction pressures of 300 and 500 MPa. Second, the sudden decrease in the stress values increases to larger strains, 0.2. Finally at 700 MPa, the foams show typical ductile metal foam behavior composing of a linear elastic deformation region followed by an increasing foam collapse region. These samples did not fracture until about large strains, 0.6. The porosity level of the foam samples sintered at 1300 °C are 61, 60 and 58% for the compaction pressure of 300, 500 and 700 MPa as seen in Table 2. The sintering duration decreased the foam porosity from 62% to 60% at a compaction pressure of 500 MPa.

The increasing sintering duration from 2 to 4 and 6 h at 1300 °C in foam samples compacted 500 MPa reverts the brittle foam behavior into a ductile one as shown in Figure 8 and 9. Foam samples sintered for 6 h shows increased yield stress as compared with that of the samples sintered at 4 h. The porosity levels of the samples compacted at 500 MPa and sintered for 4 h and 6 h are 61 and 58%, respectively. It should be noted that the initial volume percentages of the space holder is more or less reached after sintering.

Several trials were also performed by changing the initial space folder volume percentages to 52% and 72% while keeping the compaction pressure (500 MPa) and the sintering time (6 h) the same. These foam samples showed also brittle behavior, indicating that the compaction pressure and sintering time and temperature should be optimized for any specific volume percentages of the space holder.

The variation of the yield strength of the foam with porosity is shown in Figure 10. It should be noted here the data shown in this figure belong to the samples compacted at 500 MPa and sintered at 1300 °C. Therefore the variation of the porosity levels simply arises due to the change of the sintering time. It is shown in the same figure that both porosity level and yield strength are affected by the sintering time. Three percent decrease in porosity results in 20 MPa increase in the yield strength as depicted in Figure 10. The lower porosity levels naturally tend to increase the stress values since more solid is accommodated in the foam structure. However the enhanced bonding between particles at increasing sintering times may have also contribution to the foam strength.

Microscopic studies have shown that the sintered powders have Widmanstätten structure. In this structure, colonies of β lathes (bcc and rich in V) and α platelets (hcp and rich in Al) formed inside the prior β grains (Fig. 11). The percentage and thickness of β phase were measured typically 18-20% and 0.2-1 μm, respectively. The thickness of α platelets varied between 4 and 8 μm and it was also microscopically observed that the thickness of α platelets increases at and near the interparticle bond region.

Two different sizes of the pores are clearly seen in foam microstructures (Fig. 12). The larger pores, 400 micron, are due to the space holder removal

and smaller pores ranging between 10-20 micron formed between the particles. The sizes of the interparticle pores however were observed to increase at lower compaction pressures. It was also observed that high compaction pressure resulted in particle deformation as depicted in Figure 13.
Undeformed and deformed images of the foam compacted at 500 MPa and sintered at 1300 °C for 6 h are shown in Figure 14. The foam shows localized deformation starting from the mid-sections. This deformation matches with the ductile metal foam deformation. For about 60% porosity ductile foam behavior are found in the samples compacted at 500 MPa and sintered at 1300 °C for 6 h. Since higher compaction pressure may induce deformation of space holder, 700 MPa compaction pressure may be disregarded.

4 CONCLUSION

The open cell foams of Ti6Al4V alloy were prepared in the porosity around 60% using atomized spherical powders by varying the cold compaction pressure and sintering temperature and time. The green powder compacts were cold compacted at various pressures and then sintered at 1200 °C and 1300 °C for 2, 4 and 6 hours. Foams compacted at 200, 300, 500 sintered at 1200 °C for 2 h showed brittle failure, while foams compacted at 700 MPa and sintered at 1200 °C for 2 h showed ductile failure. Similarly, foams compacted at 500 MPa and sintered at 1300 °C for 4 and 6 h showed typical foam metal compression behavior composing localized deformation region and increasing plateau stress. Microscopic analysis have shown that two ranges of pore sizes: (a) larger pore sizes around 400 micron resulted from the space holder removal while (b) small size pores 10-20 micron formed between interparticle regions. The brittle foam behavior at lower compaction pressures and sintering temperature and times was attributed to the weak interparticle bonding. The results of this study were used to prepare cervical cages with a porosity of about 60% and pore size of 400 micron.

5 PHOTOGRAPHS AND FIGURES

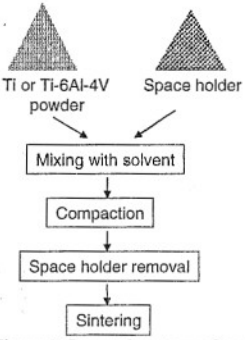

Figure 1 Processing steps of space holder method.

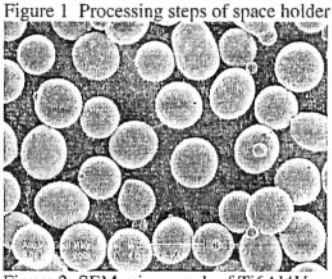

Figure 2 SEM micrograph of Ti6Al4V powder.

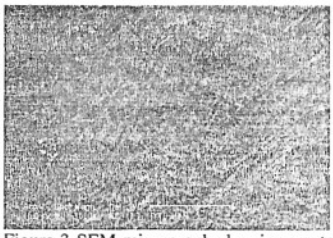

Figure 3 SEM micrograph showing martensitic α or acicula (needle like) α. microstructure of Ti6Al4V powder.

Figure 4 SEM micrograph of the space holder.

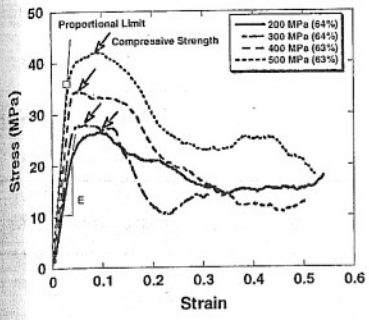

Figure 5 Compression stress-strain curves of foams (T=1200 °C, 2 h at various compaction pressures).

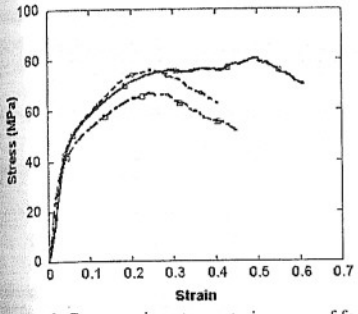

Figure 6 Compression stress-strain curve of foams cold compaction pressure at 500 MPa, T=1300 °C and 2 h.

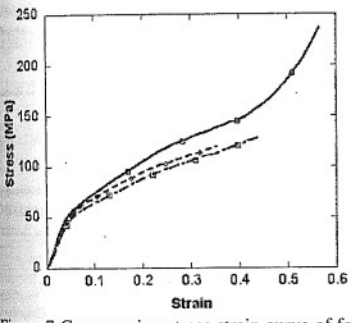

Figure 7 Compression stress-strain curve of foams cold compaction pressure at 700 MPa, T=1300 °C and 2 h.

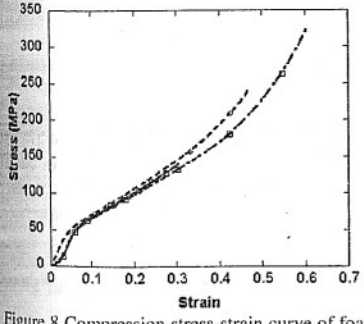

Figure 8 Compression stress-strain curve of foams cold compaction pressure at 500 MPa, T=1300 °C and 4 h.

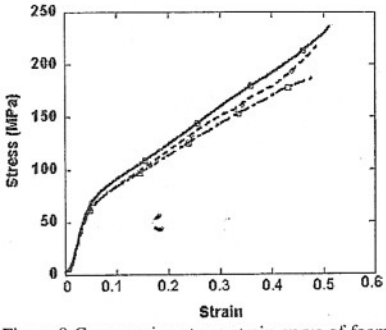

Figure 9 Compression stress-strain curve of foams cold compaction pressure at 500 MPa, T=1300 °C, 6 h <90 µm Ti6Al4V powder.

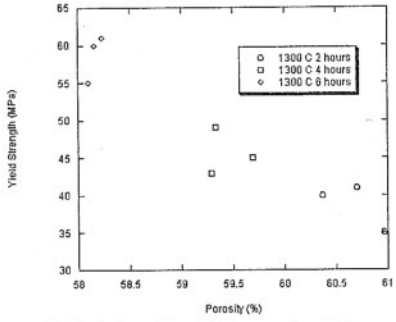

Figure 10 Variation of the yield strength with the porosity

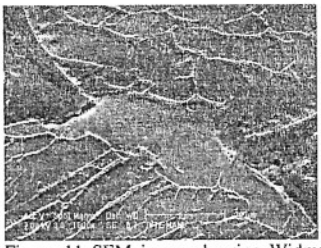

Figure 11 SEM image showing Widmanstätten microstructure of sintered foam sample.

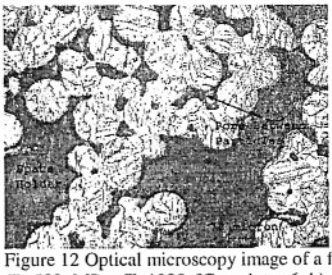

Figure 12 Optical microscopy image of a foam sample (P=500 MPa, T=1300 °C and t= 6 h) showing relatively small pores between particles and larger pores in the places left by the space holder.

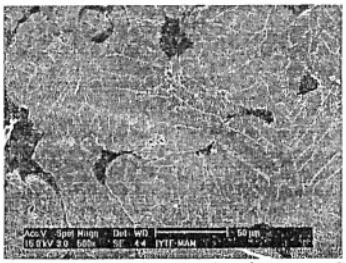

Figure 13 SEM image of a foam sample (P=500 MPa, T=1300 °C and t= 6 h) showing excessive particle deformation

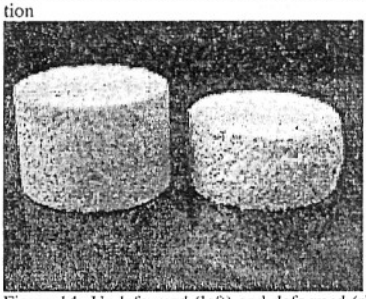

Figure 14 Undeformed (left) and deformed (right) images of the foam (P= 500 MPa, T=1300 °C, t=6 h).

REFERENCES

[1] Pillar, R. M., 1987, Porous-surfaced metallic implants for orthopedic applications. J. Biomed. Mater. Res. 21:1-3.

[2] Banhart, J., 2001, Manufacture, characterisation and application of cellular metals and metal foams. Prog. Mater. Sci. 46:559-632.

[3] Körner, C., and Singer, R. F., 2002, Processing of metal foams-challenges and opportunities. Adv. Eng. Mater. 2:159-165.

[4] Froes, F. H., 2002 Lightweight heavyweight, Metal Powder Report (www.metal-powder.net)

[5] Guden, M., Celik, E., Akar, E., Cetiner, S., 2005, Mat. Characterization: Compression testing of a sintered Ti6Al4V powder compact for biomedical applications. Elsevier 54.

[6] Clemow, A. J. T, Weinstein, A. M., Klawitter, J. J., Koeneman, J., and Anderson, J., 1981, Interface mechanics of porous titanium implants. J. Biomed. Mater. Res. 15: 73-82.

[7] Elbir, S., Yılmaz, S., Toksoy, K., Guden, M., and Hall, I. W., 2003, SiC-particulate aluminum composite foams produced by powder compacts: Foaming and compression behavior, J. Mater. Sci. 38:4745-4755.

[8] Martin, B., Stiller, C., Buchkremer, H. P., Stöver, D., and Baur, H., 2000, High purity titanium, stainless steel and superalloy parts . Adv. Eng. Mater. 2:196-199.

[9] Wen, C. E., Mabuchi, M., Yamada, Y., Shimojima, K., Chino, Y., and Asahina, T., , Processing of biocompatible porous Ti and Mg. Script. Mat. 45:1147-1153.